Advanced Engineering Informatics 52 (2022) 101596

Contents lists available at ScienceDirect

Advanced Engineering Informatics

journal homepage: www.elsevier.com/locate/aei

Full length article

Ergonomic assessment of office worker postures using 3D automated joint angle assessment

Patrick B. Rodrigues [a], Yijing Xiao [a], Yoko E. Fukumura [b], Mohamad Awada [a], Ashrant Aryal [a], Burcin Becerik-Gerber [a,*], Gale Lucas [c], Shawn C. Roll [b]

[a] Astani Dept. of Civil and Environmental Engineering, Viterbi School of Engineering, USC, Los Angeles, CA, United States
[b] Chan Division of Occupational Science and Occupational Therapy, USC, Los Angeles, CA, United States
[c] USC Institute for Creative Technologies, USC, Los Angeles, CA, United States

ARTICLE INFO

Keywords:
Ergonomic assessment
RULA
Engineering office environments
Depth camera
Computer vision
Machine learning

ABSTRACT

Sedentary activity and static postures are associated with work-related musculoskeletal disorders (WMSDs) and worker discomfort. Ergonomic evaluation for office workers is commonly performed by experts using tools such as the Rapid Upper Limb Assessment (RULA), but there is limited evidence suggesting sustained compliance with expert's recommendations. Assessing postural shifts across a day and identifying poor postures would benefit from automation by means of real-time, continuous feedback. Automated postural assessment methods exist; however, they are usually based on ideal conditions that may restrict users' postures, clothing, and hair styles, or may require unobstructed views of the participants. Using a Microsoft Kinect camera and open-source computer vision algorithms, we propose an automated ergonomic assessment algorithm to monitor office worker postures, the 3D **A**utomated **J**oint Angle **A**ssessment, 3D-AJA. The validity of the 3D-AJA was tested by comparing algorithm-calculated joint angles to the angles obtained from manual goniometry and the Kinect Software Development Kit (SDK) for 20 participants in an office space. The results of the assessment show that the 3D-AJA has mean absolute errors ranging from $5.6^\circ \pm 5.1^\circ$ to $8.5^\circ \pm 8.1^\circ$ for shoulder flexion, shoulder abduction, and elbow flexion relative to joint angle measurements from goniometry. Additionally, the 3D-AJA showed relatively good performance on the classification of RULA score A using a Random Forest model (micro averages F1-score = 0.759, G-mean = 0.811), even at high levels of occlusion on the subjects' lower limbs. The results of the study provide a basis for the development of a full-body ergonomic assessment for office workers, which can support personalized behavior change and help office workers to adjust their postures, thus reducing their risks of WMSDs.

1. Introduction

Office workers, such as engineers, architects, and designers, spend most of their work time at desks and computer stations [1–3]. Those employed in deskbound occupations assume sedentary postures for approximately 11 h per day [1]. Sedentary work postures are exacerbated by high levels of work pressure, inappropriate workplace layout and the nature of office work [4,5]. Recent shifts in work patterns due to COVID-19 have further increased the amount of sedentary work, due to reliance on computer workstations for remote work activities [6–8]. With long periods in sedentary postures, both sitting and standing, the development of work-related musculoskeletal disorders (WMSDs) becomes more likely [9]. Lack of movement, poor equipment positioning, and static, non-natural postures lead to increased neck, back, shoulder, and upper extremity discomfort in office workers [10,11]. In 2020, 21% of all injuries and illnesses leading to days away from work were due to WMSDs, with a median of 14 days away from work compared with 12 days for all other nonfatal injury and illness cases [12]. Improving office worker posture is vital to promote healthy workplaces and to minimize lost productivity due to leaves of absence [13], absenteeism [14], and presenteeism [15]. Shoulder discomfort is one of the most common types of musculoskeletal disorders among office workers [10], and studies of office workers from different countries show that people frequently complain about shoulder and arm pain [10,11,16]. Non-natural shoulder posture and inappropriate placement of the elbows are a common cause of shoulder and arm discomfort [17]. Thus,

* Corresponding author at: 3620 S. Vermont Ave, KAP 217, Astani Dept. of Civil and Environmental Engineering, Los Angeles, CA 90089, United States.
E-mail address: becerik@usc.edu (B. Becerik-Gerber).

https://doi.org/10.1016/j.aei.2022.101596
Received 24 January 2021; Received in revised form 21 January 2022; Accepted 21 March 2022
Available online 30 March 2022

shoulder and elbow joint angles are commonly used as important indicators when examining office workers' posture [10,11].

Examining joint angles and assisting office workers to improve and correct their postures at work are commonly done using self-rating questionnaires or expert observations [18,19]. Self-evaluation of posture and work-related body pain via questionnaires is the simplest and fastest way to assess workers' postures. However, this subjective method is frequently imprecise and unreliable for ergonomic interventions [18] and does not provide continuous recommendations for posture change or ergonomic interventions. Expert observations typically consists of postural evaluation and correction through real-time observations by an ergonomist, occupational therapist, or other human factors professional using tools such as the Rapid Upper Limb Assessment (RULA; [20]). The RULA is one of the most widely used observational tools for estimating risk of WMSD or musculoskeletal pain due to body postures in static or repetitive work involving the arms. Positioning of joints across the upper limb, neck, trunk, and legs are recorded, and an overall risk score (1–7) that combines all joint positioning together is often reported. Subcomponent scores for positioning of the upper limb and the combined position of the neck, trunk, and legs can also be identified, making it possible to use the RULA to estimate postural risk within each region separately.

Although both subjective and objective methods can be useful for short-term corrections to the work environment and worker posture [21], there is a lack of evidence supporting long-term adoption of ergonomic adjustments or sustained behavior changes without regular follow-ups [22,23] as workers tend to revert to their poor postures without reinforcement [18]. Reliance on ergonomic specialists to assess each worker and provide ongoing follow-ups is extremely labor-intensive, time-consuming, and typically cost prohibitive for employers [18]. Moreover, the recent shifts to remote work and work from home create further barriers to providing ongoing and expert assessment and feedback to correct poor postures. Thus, a portable and cost-effective posture monitoring system, that keeps track of office workers' postures without interrupting their daily work routine and helps office workers to adapt by providing continuous feedback to adopt better work postures without the presence of ergonomic specialists is becoming more important.

Ongoing monitoring and feedback may be best achieved using direct measurement of joint angles that can provide an intuitive output and more accurate results than other methods [19]. The two most widely used direct measurement methods include assessment using wearable sensors and cameras. Wearable sensors, such as inertial measurement units (IMUs) [24], electromyography (EMG) [25], motion capture systems [26], and reflective sensors [27], track the movement of the human body and produce body kinematics data. Wearable sensors, require direct attachment to the body and can limit the office workers' range of movement, can be burdensome to wear, and are not suitable for long-term use [18]. An alternative is unobtrusive and marker-less camera-based assessments that, when supported by machine learning algorithms, can provide automated postural assessments for workers [28–32]. Although camera-based postural assessments can be based on either RGB or RGB-D cameras, the use of RGB-D cameras has been preferred in most applications due to robustness in varying lighting conditions, calibrated scale estimates, color and texture invariance, relative ease of background subtraction, and the ability to locate body joints in the 3D-space [33,34].

The Microsoft Kinect is one of the most widely used postural sensing methods in industry and research that uses two built-in cameras: a regular RGB camera and an active sensing depth camera. The Kinect is often used as it has a built in Software Development Kit (SDK) for ease of use in skeleton detection and body joint recognition applications [35]. In these applications, the RGB and depth images captured by the Kinect camera are usually rendered and reconstructed into 3D point clouds which could be viewed from different viewpoints. RGB–D cameras have also been used to evaluate joint angles, kinematics, and range of motion of the upper limbs [36–39], sitting postures of office workers [40–43], and shoulder kinematics of computer users [44,45]. Many of these experiments were conducted in lab settings where participants were required to wear specific types of clothing like fitted tank tops [44] and participants' postures were restricted [40]; thus, the accuracy and efficacy for using RGB-D cameras in real office environments is uncertain. Additionally, despite the reported health benefits related to changing between sitting and standing postures during a work shift [46], most existing studies have primarily focused on workers who are either standing [28,31] or sitting [40,44] and, thus, the robustness of many automated assessment methods to changing working conditions and workstations setups has not been completely evaluated.

In this study, we propose an automated ergonomic assessment method, the **3D A**utomated **J**oint Angle **A**ssessment, 3D-AJA, which uses a Kinect camera and computer vision algorithms to compute office workers' upper limb joint angles and their associated postural risk based on conversion to a RULA score in both sitting and standing conditions across diverse workstation setups. Participants were advised to wear their normal clothes, normal hair styles, and behave as they normally would in completing their work tasks at a computer. Thus, the **objective** of this study was to develop an automated ergonomic assessment algorithm for office workers that could be effectively translated into realistic office environments. The following *three research questions* are answered in this study: (1) How accurate is the 3D-AJA for identifying specific body joint angles of the shoulder and arm in an office setting? (2) How does the 3D-AJA compare to the existing Kinect SDK body joint capture method for body joint angle measurements? (3) How might the 3D-AJA support assumptions of postural risk as would be manually assessed using the RULA? The remainder of the paper is organized as follows. Section 2 presents an overview of the relevant literature. The proposed methodology of this study is described in Section 3. Section 4 and Section 5 presents the results and discussion, respectively. Finally, conclusions are presented in Section 6.

2. Literature review

Camera-based ergonomic assessments can be performed either in 2D using regular cameras [47–49] or in 3D using RGB-D cameras, such as ranged cameras [50] and Kinect cameras [44,51]. Previous studies investigated the application of camera-based ergonomic assessments on workers in different settings such as industrial [52–54], manufacturing [27,55,56], assembly [30,57], and construction [58,59]. For example, studies evaluated the validity of Kinect camera for posture assessment in lab environments where participants were asked to perform weightlifting tasks [27,59,60], bending [30,61], or moving upper and lower limbs in front of the camera [35,37,62]. Other studies tested the performance of Kinect camera on worker evaluation in real factory workplaces, such as using assembly tables [55] and in a fabric plant [54]. The performance of these evaluations differs when lab-based and workplace-based assessments are compared. For example, Plantard et al. [27] compared the performance of Kinect camera for box lifting tasks in a lab environment and car seat assembly in a real car manufacturing factory and found that the strength of agreement between RULA scores computed from Kinect data and expert observations in real work conditions was around 80% in the lab, which was higher than 70% in a factory.

However, the outcomes of the methods developed in the above-mentioned studies may be different when these methods are applied for posture monitoring of office workers. Compared to construction workers who stand and perform strenuous and/or repetitive tasks [32], office workers sit or stand and perform repetitive tasks with a smaller range of movements [16,63]. Additionally, given that part of the office workers' lower body may be occluded by their workstations, it is possible that the performance of camera-based postural assessment methods based on full body tracking may be compromised in an office setting due to occlusion [27,64]. For example, the Kinect Software Development Kit (SDK), a built-in body joint and skeleton detection

function in the Kinect camera, works better when the participant is standing in front of the camera with all body parts exposed [58]. In other words, the Kinect SDK skeleton tracking does not usually work well when the participant sits behind the desk with parts of their body occluded [65], which requires certain remedial measures to overcome challenges such as the lack of accuracy when the participant being tracked is not facing the camera directly or when parts of the body are not visible to the camera [35].

Previous studies developed applications based on RGB-D cameras to keep track of postures of office workers [66–68]. Several studies focused on the sitting postures of office workers [40–43] and used the Kinect SDK. Even though moderate-to-high correlations have been found between the Kinect angles and goniometer angles in these studies, in most cases, the workstation setups and the requirements on the participants postures were too restrictive to be representative of real office environments. Examples include the use of workstations without computers and other objects, combined with participants following predetermined protocols and having sensors attached to their bodies [40], the need to use markers to detect participant's body parts and have sensors attached to the participant's body [43]. Because shoulder and elbow joint angles are important indicators of office workers' health [10,11], other studies used Kinect SDK to monitor the joint angles [36,37], kinematics [38], and range of motion [39] of upper limbs at standing postures. For 0° and 90° shoulder flexion and abduction angles, Kinect camera measurements have shown a correlation coefficient of 0.76–0.98 with goniometry measurements [28], but further studies are needed to evaluate its performance in a broader range of angles for these joints. Studies also used Kinect SDK to perform postures assessment of office workers whose predominant mode of work was using computers [44,45,69]. Again, although moderate-to-high correlations have been found between Kinect angles and goniometer angles, as it was the case in many studies focusing on sitting postures, the boundary conditions in these studies may limit their validity in real world conditions. For example, some of the existing studies have limited the range of postures the participants can use during the experiments and have required participants to wear fit clothes to allow the attachment of sensors to the participants' bodies [44]. Table 1 presents a summary of some of the existing studies that involve the automated assessment of postural risk in various workplaces.

While the Kinect SDK has been tested for ergonomic assessment in office settings with the above limitations, with the application of deep learning in computer vision, postural detection with 2D images has attracted attention and is developing rapidly [71]. Automated algorithms not only have the potential to improve upon the challenges faced in previous studies, but these advanced techniques may also serve as the foundation for developing a method for the ongoing assessment and feedback required to support behavioral change in office workers. There are two categories of emerging algorithms. First, direct body joint detection algorithms [72–74] capture the body joints directly and connect the detected joints to compute body joint angles. Second, body part parsing and segmentation algorithms [75,76] create pixel-level human body part segmentations and classify pixels in the 2D image into categories that belong to different body parts. These algorithms have been applied to a variety of body movement tracking, such as with athletes [77] and construction workers [78]; however, to the best of the authors' knowledge, these algorithms have not been applied in an office context for joint angle estimations or overall posture assessment.

To examine the automated assessment of office worker posture, we evaluated a combination of two algorithms, a direct body joint detection algorithm, OpenPose [74], and a body part segmentation algorithm, Weakly and Semi-Supervised Human Body Part Parsing (WSHP) [76]. OpenPose achieves a balance between accuracy and computational speed to provide separate joint estimation for the body, foot, and facial key points, all of which are suitable for office workers when part of their body is occluded behind workstations. WSHP provides pixel-level human body segmentation, which helps automatically recognize different body parts, providing the basis for body joint angle calculations. Together these algorithms can more precisely determine the position of body parts and avoid the limitations of using 3D body joint coordinates from Kinect SDK alone. However, since 2D outputs from the OpenPose and WSHP may be limited to compute human body joint angles in 3D space, we propose a novel algorithm, 3D-AJA, that combines 3D data from Kinect cameras with the 2D outputs of the selected computer vision algorithms to determine body joint angles used for RULA scores calculations. This algorithm serves as our first step toward developing an automated system to conduct ongoing postural risk evaluations for office workers.

3. Materials and methods

3.1. Automated joint angle assessment – 3D-AJA

Our automated ergonomic assessment algorithm combines open-source computer vision algorithms and a novel body joint angle calculation algorithm. The process involves body joint detection and body part segmentation in RGB images, image registration, merging of RGB and depth images to construct a 3D human body point cloud model, and calculation of body joint angles using the 3D point cloud. Fig. 1 presents a flowchart of the proposed body joint angle calculation algorithm, the 3D-AJA.

The RGB images and depth images were collected using a Microsoft Kinect for Windows V1 camera (step 1.1 in Fig. 1). Two open-source computer vision algorithms, OpenPose [74] and WSHP [76], were

Table 1
Comparison of performance metrics for existing automated postural assessment in the workspace using computer vision.

Study	Camera	Assessment	Working condition	Boundary conditions	Performance metrics
Seo, S. Lee [31]	RGB	OWAS (Ovako Working Posture Analyzing System	Standing, back-bending, arm-raising, knee-bending	Laboratory, limited number of postures (4), full body, no occlusion	Accuracy = 89%
Dzeng et al. [32]	3 × RGB-D	OWAS (4 action levels)	Lifting, assembly, hammering, tiling	Laboratory, eventual partial occlusion of lower limbs	Accuracies between 48.4% and 93.9%
Bhatia et al. [40]	RGB-D	Elbow flexion/extension, Knee flexion/extension	Sitting	Laboratory, sensors attached to the participants, no objects on workstation, controlled lighting	RMSE ranging from 9.7° to 15.4° Correlation coefficient ranging from 0.6 to 0.9
Xu et al. [44]	RGB-D	Shoulder flexion/extension, axial rotation, and abduction/adduction	Sitting	Laboratory, controlled clothing (tank-tops), occluded lower limbs.	RMSE ranging from 6.4° ± 0.9° to 27.3° ± 15.8°
Abobakr et al. [51]	RGB-D	RULA (grand score)	Various	Laboratory, full body, eventual partial occlusion of body parts	MAE = 3.19° ± 1.50° Accuracy = 89%
Manghisi et al. [61]	RGB-D	RULA (grand score)	15 selected postures involving sitting, kneeling, among others	Laboratory, controlled lighting, full body, no occlusion	proportion agreement index = 0.96, k = 0.84
Li et al. [70]	RGB	RULA (4 action levels)	Lifting Sitting/Standing using Human 3.6 data	Laboratory, full body, no occlusion	F1-score = 0.79 (lifting) F1-score = 0.93 (Human 3.6)

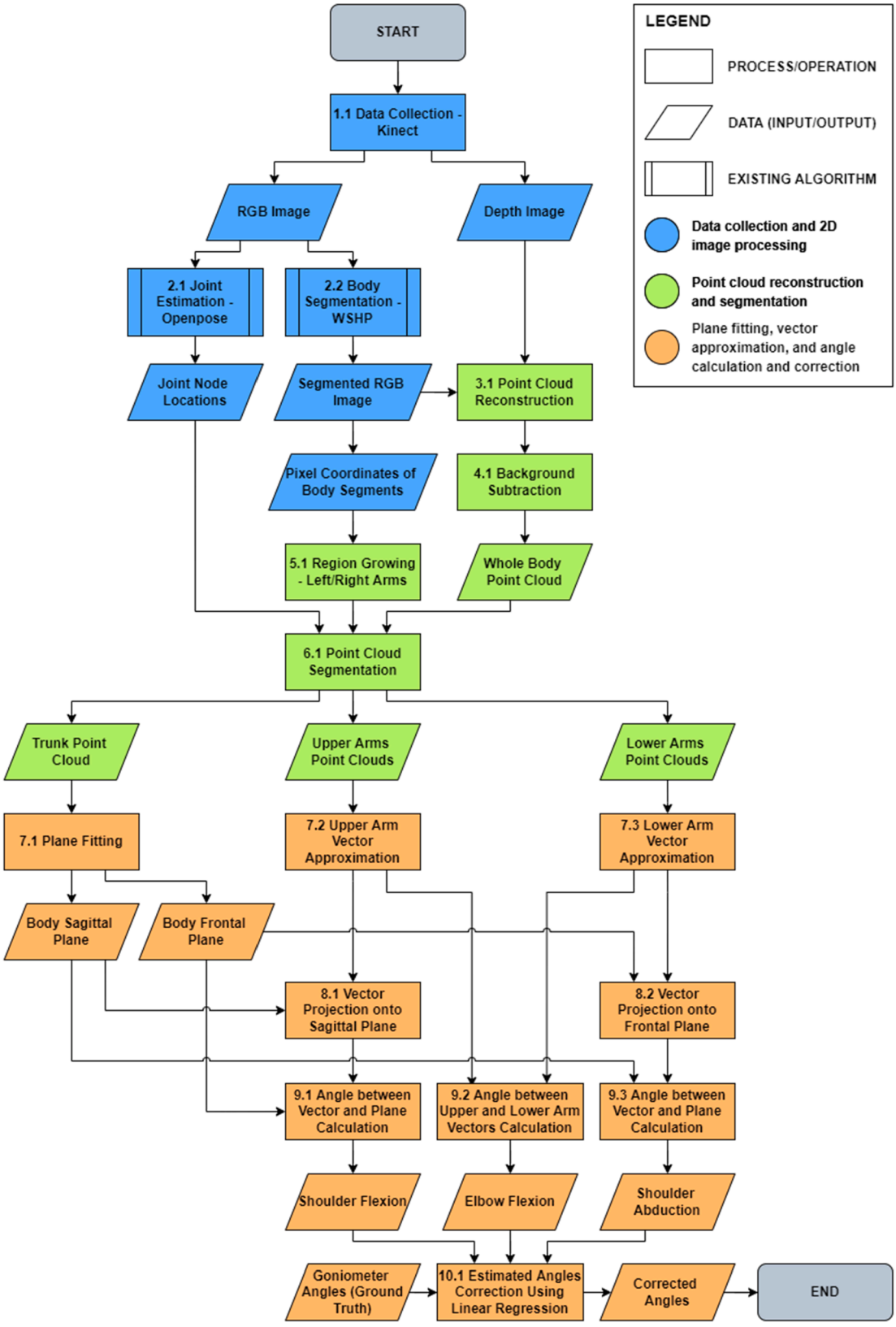

Fig. 1. Flowchart of the 3D-AJA.

combined for body joint detection and body part segmentation in RGB images (steps 2.1 and 2.2 in Fig. 1, respectively). OpenPose uses a bottom-up approach to generate Part Affinity Fields (PAF) to associate a body part to an individual. PAFs are a set of 2D vectors that encode the location and orientation of a human body part [74]. WSHP uses key point annotation to perform per-pixel part segmentation. The key idea is to exploit anatomical similarity among humans to transfer the parsing results from one person to another with a similar pose [76]. These two

algorithms take the RGB images as inputs from the Kinect camera positioned in front of the participant. OpenPose outputs 2D coordinates of detected body joints (Fig. 2 (a)) and WSHP outputs pixel-wise points that are identified as different body parts (Fig. 2 (b)). The detected body part pixels from WSHP outputs are labeled as upper arms (yellow), lower arms (purple), and trunk (green) in the RGB images.

The RGB and depth images from Kinect were overlaid on global coordinates to construct 3D point clouds (step 3.1 in Fig. 1, results in Fig. 3). The sample size of each point cloud in this study was 0.6 in (1.5 mm) and, on average, each point cloud had 250,000 points. Further information regarding camera alignment and 3D point cloud generation can be found in MathWorks [79]. Background subtraction was performed using the Kinect SDK to eliminate noise from the background and to keep points located on or close to the human body (step 4.1 in Fig. 1, results in Fig. 4 (a) and (b)). From the 3D human body point cloud model, separate point clouds for upper arms, lower arms, and trunk were extracted (step 6.1 in Fig. 1). It was found that the WSHP algorithm could mismatch the points from the arms and assign incorrect right arm labels to left-arm points and vice versa. To solve this problem, region growing [80] was used on the upper arm and lower arm point clouds separately to differentiate the left and right arms (step 5.1 in Fig. 1). Region growing is an algorithm that picks a random pixel as a region start point inside the RGB image, examines the Euclidean distance between neighboring pixel points and start point and determines whether the pixel neighbors belong to the same region.

Next, the novel body joint angle calculation algorithm was designed to calculate shoulder flexion, shoulder abduction, and elbow flexion joint angles by replicating manual goniometry procedures [81]. The demonstration of shoulder flexion, shoulder abduction, and elbow flexion is shown in Fig. 5. Shoulder flexion/extension is the respective movement of the arm up/down in front of the body in the sagittal plane, and shoulder abduction/adduction is the respective movement of the arm away from and toward the side of the body in the frontal plane. Elbow flexion/extension refers to the respective movement of the elbow joint that decreases or increases the joint angle relative to a straight arm position. Manual joint angle measurements using a goniometer are conducted following a 4-step procedure: (1) identify designated parts of the body for measurements, (2) approximate the location of bones, the skeletal joint, and the body planes, (3) project the location of bones in space onto the body planes, and (4) measure projected angles with the goniometer centered over the joint as the axis of movement. We developed our body joint angle calculation algorithm to follow the same procedure, where the location of arm bones, shoulder and elbow joints, and frontal and sagittal planes of the trunk were found first. Then, the locations of upper and lower arms were approximated based on the orientation of the arm skeleton, and the shoulder and elbow joint angles were measured based on the relative angle between arm skeletons and trunk planes.

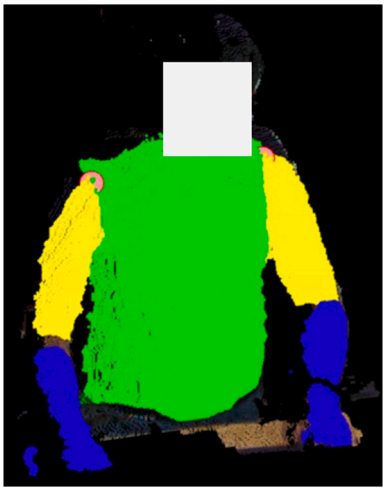

Fig. 3. 3D human body point cloud model.

The trunk frontal plane was approximated by fitting a plane amongst all points labeled as the trunk with the least square of the normal distance from all trunk points to the plane (step 7.1 in Fig. 1). The body sagittal plane was obtained by forming a plane along the direction perpendicular to the vector connecting the two shoulder joint points output and aligned with the normal vector on the body frontal plane (Fig. 6). Upper arm skeleton locations of left and right upper arms were found by fitting two lines in the 3D space among all the points identified as left and right upper arms. The equation of each line in space was calculated using the least square approximation method, followed by its transformation into a vector in space for joint angle calculations. The same method was used to find the approximate skeleton location of the lower arms (step 7.3 in Fig. 1). The upper arm vectors pointed from the shoulder joint to the elbow joint and the lower arm vectors pointed from the elbow joint to the wrist joint.

The approximated arm vectors, trunk frontal planes, and sagittal planes were used for body joint angle calculations. Shoulder flexion angles were obtained by projecting the upper arm vector in space to the body sagittal plane and calculating the angle between the projected vector and the body frontal plane (steps 8.1 and 9.1 in Fig. 1, respectively). Shoulder abduction angles were obtained by projecting upper arm vectors in space to the body frontal plane and calculating the angle between the projected vector and the body sagittal plane (steps 8.2 and 9.3 in Fig. 1, respectively). Elbow flexion angles were calculated from the angle between the upper arm and lower arm vector in the 3D space (step 9.2 in Fig. 1). Total processing time for each frame was around 80 s on an Intel® Xeon® E5420 @ 2.50 GHz CPU with 16 GB RAM.

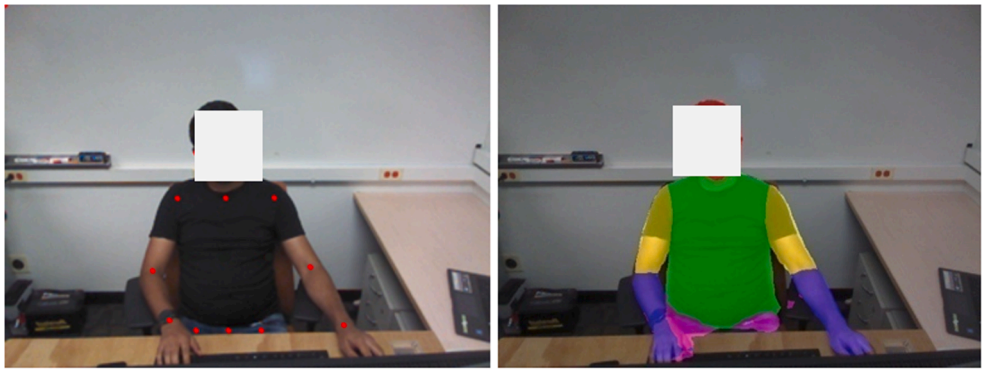

Fig. 2. (a) OpenPose sample output and (b) WSHP algorithm sample output (right).

Fig. 4. Point cloud (a) before and (b) after background subtraction.

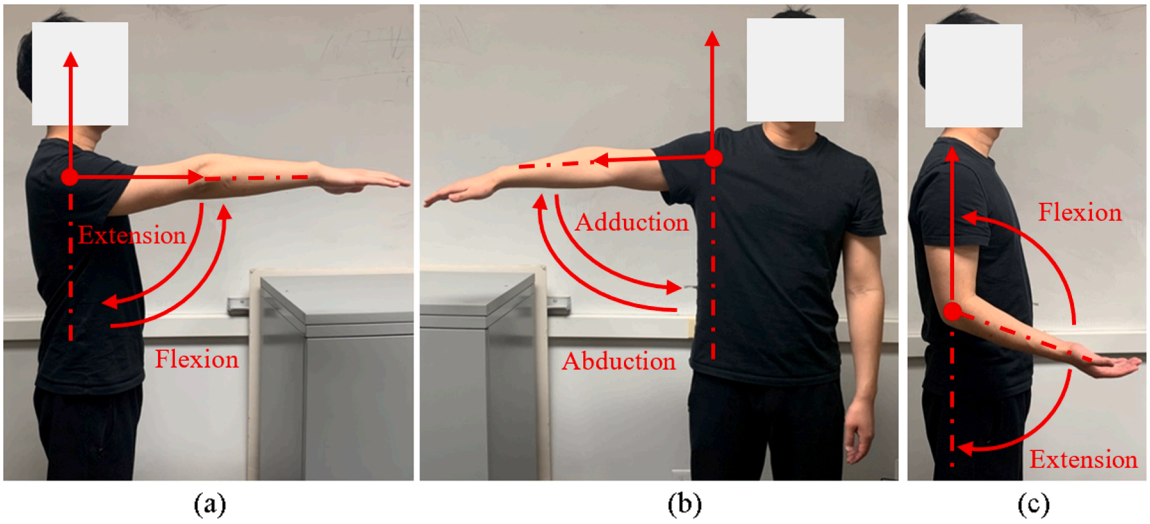

Fig. 5. (a) Shoulder flexion, (b) shoulder abduction, (c) elbow flexion.

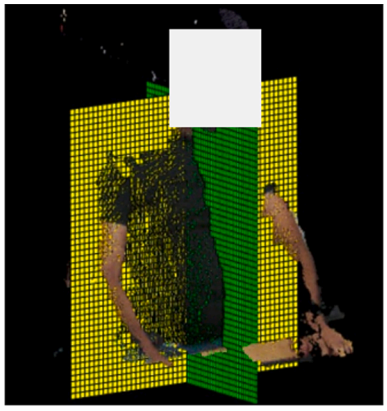

Fig. 6. Body frontal plane (yellow) and sagittal plane (green) approximation. (For interpretation of the references to color in this figure legend, the reader is referred to the web version of this article.)

3.2. Algorithm evaluation

An experimental study was conducted to obtain a postural dataset from a group of healthy participants while working in six different computer workstation set-ups. Using this postural dataset, the 3D-AJA was evaluated and compared to goniometry measurements and the Kinect SDK. The experimental conditions were approved by the University's Institutional Review Board and all participants provided informed consent before any data collection.

3.2.1. Experimental setup

The experiment was conducted using a standardized office workstation that included a fully adjustable chair, an adjustable-height desk, and a monitor, keyboard, and mouse that could each be moved (Fig. 7). Previous studies recommended placing the camera directly in front of the participant and within approximately 16 feet (4.88 m) to provide the best accuracy for determining body angles and use of the depth channel [35,40,44,62]. Therefore, in this study, both RGB and depth images were captured using a Kinect camera mounted on a tripod 6 in. (15.24 cm) behind a computer monitor directly in front of the participant, at an approximate distance of 6 feet (1.83 m) from the participant. A MATLAB script was written to process Kinect data into files containing Kinect default RGB images (480x640 resolution), Kinect default depth images (480x640 resolution), skeleton joint coordinates from Kinect SDK, and relevant metadata. Data files were recorded twice every second, and all the data points of a snapshot were then combined into a single file to ensure synchronization. An RGB web camera was also mounted on the wall to the right of the participant and continuous video recording was completed throughout the experiment. This video recording provided

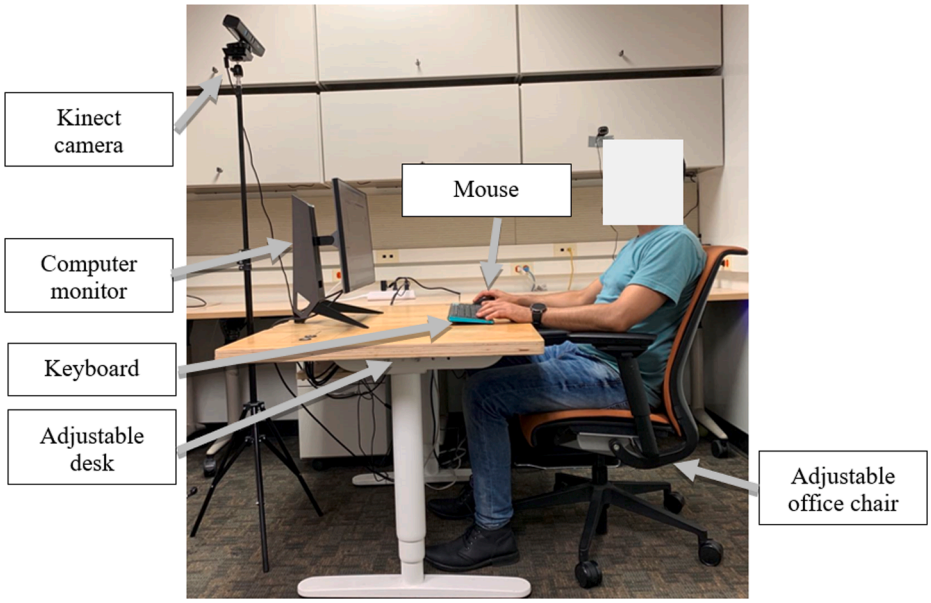

Fig. 7. Experiment setup.

additional input for the team to identify potential data errors and improve the expert coding of RULA scores for comparison to the algorithm-calculated risk scores.

3.2.2. Data collection

Twenty participants (8 females and 12 males) without any known musculoskeletal disorders or limitations of upper body range of motion were recruited. All participants were intense computer users, 19 were right-handed, and all wore clothing and had hair styles that would be typical for conducting their work. At the outset of the experiment, each participant was introduced to the workstation and all possible adjustments, including the chair height, seat depth, armrest height, back support, desk height, monitor height and tilt, and mobility of the keyboard and mouse. The data collection consisted of two one-hour observations. The first one-hour observation had six 10-minute conditions, including (a) sitting – self-selected, (b) sitting – ideal, (c) sitting – poor, (d) standing – self-selected, (e) standing – ideal, (f) standing – poor. Workstation adjustments for each of the ideal and poor conditions were made by the experimenter as described in Table 2 and pictured in Fig. 8 (a)-(f). During the second hour, participants were allowed to adjust the workstation to any position preferred.

During the first hour, participants worked in each of the six workstation conditions (Fig. 8 (a)-(f)) for 10 min per condition. Participants were randomly selected to start in either sitting or standing for the first three set-ups before alternating to the opposite position for the three final conditions. Each set of three conditions started with the self-selected set-up, followed by the ideal and poor conditions. A 12-inch (30.48 cm) round goniometer was used for manual measurement of body joint angles. Each goniometry measurement consisted of bilateral readings of shoulder flexion, shoulder abduction, and elbow flexion for both the left and right sides of the body using standard goniometric procedures. Ten manual goniometry measurements were obtained during this process, first after the self-selected set-up, then at the start and conclusion of both the ideal and poor conditions. At each time point, participants were asked to maintain a static posture while goniometry measurements were obtained for shoulder flexion (SF), shoulder abduction (SA), and elbow flexion (EF) on the left and right arms. During the second hour, manual goniometry measurements were performed once every 15 min for a total of 4 additional measurements.

Table 2
Self-selected, ideal, and poor sitting/standing workstation conditions for the first hour.

(a) Sitting – Self-selected	• The participant adjusts all components of the workstation to his/her most comfortable or preferred position.
(b) Sitting – Ideal	• Knees, hips, elbows at approximately 90° flexion • Shoulders are relaxed, at neutral flexion/abduction • Elbow rests placed under participant's elbow, allowing for the arm to rest without shoulders hiking up • Monitor height is at eye level • Seat pan allows for 1.5 in. (3.81 cm) width space between the back of knees and edge of the chair
(c) Sitting – Poor	• Desk height lowered to encourage full extension of elbows • Elbow rests are adjusted so the arms are not supported • Monitor height lowered and pushed to one side to encourage neck forward and lateral flexion • Keyboard away from the participant's body to encourage elbow extension
(d) Standing – Self-selected	• The chair is removed, and the participant adjusts the desk height and all other items to his/her preferred position.
(e) Standing – Ideal	• Standing with both feet on the floor • Elbow at approximately 90° and shoulders are relaxed, in neutral flexion/abduction • Monitor height is at eye level • Neck and spine in a neutral position
(f) Standing – Poor	• Desk height lowered to encourage full extension of elbows • Monitor height lowered and pushed to one side to encourage neck forward and lateral flexion • Keyboard away from the participant's body to encourage elbow extension

3.2.3. Data processing and analysis

The three joint angles on both the left and right sides were measured 14 times for each participant, resulting in a total of 1,680 individual measurements across all participants, conditions, and joints. Error in manual goniometry was discovered during data cleaning and processing. After checking the noted goniometry angles and corresponding RGB images at the same time frame, 11 measurements were eliminated from the analysis due to the mismatch and obvious large discrepancies between the RGB images and corresponding goniometry measurements. These discrepancies were due to a participant moving between the measurement of their joint angles for their left and right sides, and/or due to human error during the transferring of the goniometer measurements to the assessment sheet. Next, body joint angles were calculated using the 3D-AJA as explained in Section 3.1, and skeleton joint

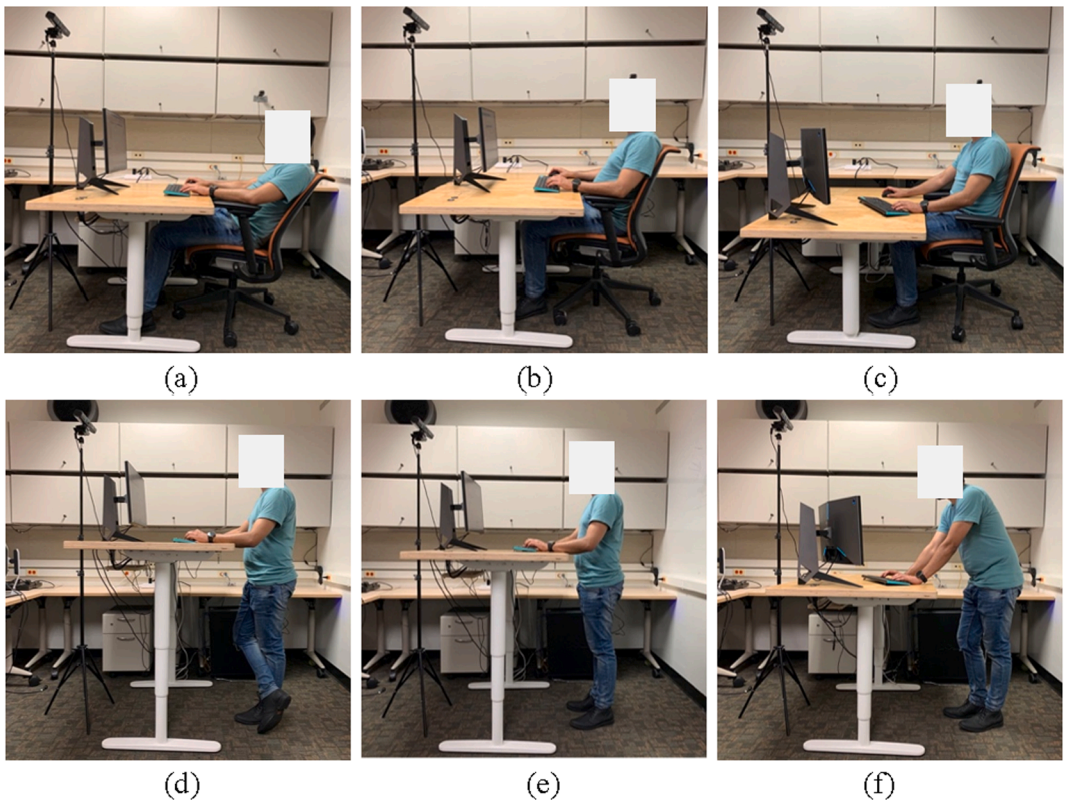

Fig. 8. Sample images of the six workstation adjustments tested including sitting in (a) self-selected, (b) ideal, and (c) poor set-ups, and standing in (d) self-selected, (e) ideal, (f) poor set-ups.

coordinates from Kinect SDK were used to calculate body joint angles following ISB recommendations [82] and Xu et al [44].

Raw output from the algorithm and the Kinect SDK was calibrated by fitting a linear regression model with goniometry measurements and adjusting the raw algorithm and Kinect SDK output based on this model to eliminate systematic error in the data (step 10.1 in Fig. 1). Mean Absolute Error (MAE) and Pearson correlation (r) were calculated to compare the performance of the algorithm and the Kinect SDK relative to the goniometry measurements. Specifically, MAEs relative to the goniometry measurements were compared between the algorithm and Kinect SDK using independent sample t-tests. Comparisons of the MAEs between sitting and standing conditions and between the first and second hours of data collection were also conducted using an independent sample *t*-test. Correlation analyses relative to the goniometry measurements were performed for both the algorithm and Kinect SDK and Pearson r correlation coefficients were calculated. All statistical testing was conducted using MATLAB, and statistical significance was set at $p < 0.05$.

3.2.4. *Evaluation of the proposed method for estimating postural risk*

Finally, to examine the utility of the 3D-AJA for assessment of potential postural risks associated with the participant's upper limbs, we calculated the RULA upper limb component score (i.e., RULA score A) using the estimated angles (i.e., shoulder flexion, shoulder abduction, and elbow flexion) plus an additional feature that indicated whether the participant was sitting or standing. To determine the RULA score A, one needs to locate the positions of upper arms, lower arms, wrists, and the wrist twist, then determine the individual scores associated with the locations of these members after eventual adjustments, and finally use these four individual scores to identify the RULA score A in its associated table. For an explanation of RULA score A, please refer to [20].

The complete evaluation of RULA score A for arm and wrist analysis [20] requires nine features: positions of upper arms, lower arms, wrists, the wrist twist, and 5 eventual adjustments. However, extracting all 9 features from the RGB-D data, particularly those associated with wrist position, is challenging in real environments because the camera positioning or resolution may not be able to capture hand location appropriately [70] or because wrists may be located outside the camera's field of view due to the user's movement during different office tasks. To overcome this challenge, we evaluated the potential of using Machine Learning models to provide a consistent assessment of RULA score A using the arm and shoulder joint angles which are generally visible in the camera's field of view even when the extremities might not be visible. For these models, the three joint angles and the participant's condition (sitting/standing) were used as the input features and the RULA score A determined by the ergonomists as the class label. Fig. 9 presents the overall process for training and testing the selected models.

For each participant, approximately 120 frames were selected from the first hour of data collection (1 frame every 30 s), totaling about 2,400 frames. The decision to select the first hour of data collection aimed at including all six combinations of workstation setups and working conditions, as presented in Table 2. Two occupational therapists with experience in ergonomic assessment conducted the RULA for each frame. The upper limb was scored based on positioning of the right arm due to the ability for the expert observers to review the additional RGB video positioned lateral to the participant as needed.

Before training and testing the models, the datasets were cleaned to remove instances that contained missing values for any of the features and eventual outliers. Then, the cleaned datasets were randomly partitioned into two sets, one for training and one for testing the ML models for seven different folds. As a result of the verification of highly imbalanced datasets for both the 3D-AJA and the SDK, it was necessary to oversample the minority classes in the training datasets, which was done using the Synthetic Minority Oversampling TEchnique (SMOTE) algorithm [83]. Finally, the testing dataset was used to assess the quality of the trained models.

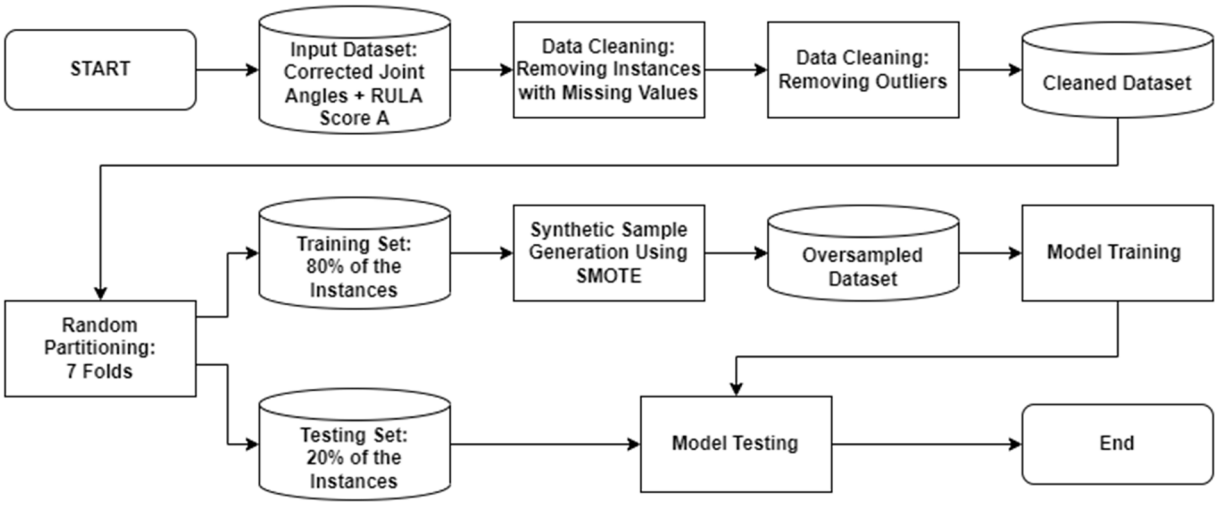

Fig. 9. Flowchart of the training and testing methods for the selected models.

Table 3 presents a summary of the distribution of the RULA score A classes for the training and testing datasets for the 3D-AJA and the Kinect SDK. As Table 3 shows, there is a high imbalance in both datasets (3D-AJA and Kinect SDK), with classes 1, and 6–9 having the lowest number of instances as compared to the majority classes represented by classes 2 and 3. Classes 4 and 5 also represent minority classes, although the imbalance ratios of these classes relative to the majority classes are not as pronounced as it is for classes 1, 6, and 7. Possible explanations for this observation is related to the RULA score A table itself and the set of possible workstation adjustments likely to be found in an office workspace. Out of the 144 possible combinations of arm and wrist angles, only one results in a RULA score A of 1 [20]. Alternatively, to reach the most extreme RULA scores A from 6 to 9, the workers would need to be sitting or standing is positions not likely to be found during computer work in a common office space. Another observation in Table 3 is that, for the 3D-AJA, no instances belonging to class 6 were found in the dataset. For the Kinect SDK, only one instance belonging to class 6 was captured, although it was dropped because the SMOTE algorithm could not be applied to it. No instances were classified as classes 8 or 9 for both the 3D-AJA and the Kinect SDK. Finally, Table 3 shows that, due to the observed class imbalances in the original datasets, the SMOTE algorithm was applied to classes 1, 4, 5, and 7.

Imbalanced datasets are a common problem in many machine learning applications and call for remedial measures and alternative analysis metrics to reduce for the potential biases of classifying the minority classes under the majority classes due to the unequal distribution of the data among the multiple classes in the dataset [84–87]. As Table 3 shows, the majority classes 2 and 3 account for almost 90% of the instances after data cleaning while the most extreme classes 1, 6, 7, 8, and 9 together account for less than 1% of the instances in the datasets for both the 3D-AJA and the Kinect SDK. In this study, three main remedial solutions were tried to improve the classification performance of the resulting models including (1) undersampling the majority classes, (2) oversampling the minority classes, and (3) a mix of undersampling the majority classes and oversampling the minority classes to decrease the data imbalance levels. Out of the three methods, the one that resulted in the best performance for the classification models was oversampling the minority classes with the SMOTE algorithm [83].

To compare the qualities of the classification models provided by joint angles from the 3D-AJA and the Kinect SDK, nine machine learning models were evaluated. These models included the lazy classifiers k-Nearest Neighbor, KStar, and Locally Weighted Learning using the J48 tree, the Naïve Bayes classifier, the Bayes Network classifier with Bagging, the Random Tree classifier with Bagging, the rule-based classifier PART with Bagging, the Multilayer Perceptron classifier with the MultiClass Classifier (metaclassifier), and the Random Forest Classifier. All models were trained and tested using the Waikato Environment for Knowledge Analysis (WEKA), version 3.8.5 [88].

Given that the classifications dealt with highly imbalanced datasets, using accuracy as the main performance metric to compare the quality of the models could provide misleading results. This is because a model may achieve a high accuracy due to a relatively good performance in the classification of the majority classes even if the model has a poor performance in the classification of the minority classes, which is known as the "accuracy paradox" [89]. Researchers suggest using other performance metrics to assess the quality of the ML models used to train and test imbalanced datasets [85,90,91]. Some of the most used metrics include the geometric mean (G-mean) of sensitivity [True Positive (TP) Rate] and specificity [1 – False Positive (FP) Rate], and the areas under the Receiver Operating Characteristic (ROC) curve. Alternatively, it is

Table 3
Distribution of instances among the RULA scores A classes.

Class (RULA score A)	3D-AJA				Kinect SDK			
	Initial	% of the dataset	Training	Testing	Initial	% of the dataset	Training	Testing
1	11	0.5%	51*	11	8	0.4%	51*	8
2	1175	50.8%	945	230	1081	50.6%	881	200
3	902	39.0%	715	187	830	38.8%	653	177
4	175	7.6%	181*	87	172	8.0%	180*	83
5	49	2.1%	116*	25	43	2.0%	78*	25
6	–	–	–	–	1	0.0%	–	–
7	2	0.1%	24*	2	2	0.1%	24*	2
8	–	–	–	–	–	–	–	–
9	–	–	–	–	–	–	–	–

* Oversampled classes using the SMOTE algorithm. No instance was used in both training and testing datasets for the same fold.

possible to use precision-recall metrics, which also include the F-score and the area under the precision-recall curve (PRC). Thus, for this study, accuracy was not used as the main performance metric to assess the quality of the proposed models, but rather precision-recall metrics and sensitivity-specificity metrics were used. Specifically, F1-score and G-mean were selected as the main indicators of performance for the selected models. The F1-score combines precision and recall into a single value that indicates the "goodness" of a model, even in face of class imbalances [85]. Alternatively, the G-mean was proposed to deal with imbalanced datasets by balancing out the performance of the model in terms of both the positive and the negative classes [91]. The formulas used for these metrics are presented in Eqs. (1)–(6).

$$Accuracy = \frac{TP + TN}{TP + TN + FP + FN} \tag{1}$$

$$Precision = \frac{TP}{TP + FP} \tag{2}$$

$$Recall(Sensitivity) = \frac{TP}{TP + FN} \tag{3}$$

$$Specificity = \frac{TN}{TN + FP} \tag{4}$$

$$F1 - score = \frac{2 \times Precision \times Recall}{Precision + Recall} \tag{5}$$

$$G - mean = \sqrt{Sensitivity \times Specificity} \tag{6}$$

where TP = True Positive cases, TN = True Negative cases, FP = False Positive cases, and FN = False Negative cases.

4. Results

Table 4 presents the MAEs and their respective standard deviations between the paired observations of the 3D-AJA and the Kinect SDK angles to the goniometer angles for shoulder flexion, shoulder abduction, and elbow flexion across all workstation conditions. As Table 4 shows, overall, the MAE for the algorithm was significantly different than the Kinect SDK for shoulder flexion ($6.3^\circ \pm 5.7^\circ$ vs. $8.3^\circ \pm 7.2^\circ$, respectively, $p < 0.001$) and elbow flexion angles ($8.5^\circ \pm 8.1^\circ$ vs. $18.2^\circ \pm 16.0^\circ$, respectively, $p < 0.001$), although for some postural conditions (sitting ideal, sitting poor, standing self-selected, and standing ideal) no significant differences were found for shoulder flexion angles. For shoulder abduction, overall, no significant differences were found between the MAEs of the 3D-AJA ($5.6^\circ \pm 5.1^\circ$ vs. $6.2^\circ \pm 6.4^\circ$, respectively, $p = 0.113$).

We also compared the MAEs for each joint angle estimate using the 3D-AJA and the Kinect SDK between the first and second hours and between the overall sitting and standing positions ($\alpha = 0.05$). For the 3D-AJA, the only significant difference between the MAEs occurred for shoulder abduction between the overall first and second hours ($5.1^\circ \pm 4.2^\circ$ vs. $6.8^\circ \pm 6.7^\circ$, respectively, $p < 0.001$). However, for the Kinect SDK, there were significant differences between the MAEs for shoulder abduction between the overall sitting and standing positions ($6.9^\circ \pm 7.1^\circ$ vs. $4.5^\circ \pm 3.5^\circ$, respectively, $p < 0.001$), and between the overall first and second hours (5.7 ± 5.7 vs. 7.4 ± 7.7, respectively, $p = 0.007$). Also, for the Kinect SDK, significant differences between the MAEs for elbow flexion between the overall first and second hours of data collection were detected (19.7 ± 16.4 vs. 14.4 ± 14.2, respectively, $p < 0.001$).

Pearson correlation coefficients between the calculated body joint angles and goniometry measurements are presented in Table 5. For almost all cases, the measures obtained using the algorithm were more strongly correlated with the goniometry measurements than the measures obtained using the Kinect SDK. The only condition in which the Kinect SDK showed a meaningfully stronger correlation with the goniometry measurements than the 3D-AJA was the standing ideal condition (0.63 vs. 0.52, respectively). Across the varied conditions tested in the first hour, there were significantly strong correlations between the algorithm calculated joint angles and goniometry measurements at 0.79 for shoulder flexion, 0.77 for shoulder abduction, and 0.90 for elbow flexion. Alternatively, the Kinect SDK showed a weak correlation for elbow flexion (0.30) and moderate correlations for shoulder flexion (0.61) and shoulder abduction (0.61). Similar results were noted across the measures conducted for each method during the self-selected work behaviors in the second hour and the overall results throughout all conditions during both the first and second hours of data collection as shown in Table 5.

Out of the nine selected machine learning models, the model which provided the overall best performances for both the 3D-AJA and the Kinect SDK was the Random Forest. The confusion matrices and performance metrics for all classes in the Random Forest models are presented in Tables 6 and 7, respectively, for both the 3D-AJA and the Kinect SDK. As Table 7 shows, the F1-scores of all classes in the model from the 3D-AJA data are at least 0.700, and the G-means of all classes are higher than 0.840. Alternatively, the model using the Kinect SDK data shows relatively lower F1-scores and G-means for some of the

Table 4
Comparisons of mean absolute error (MAE) relative to goniometry measurement between the 3D-AJA and Kinect SDK, in °.

	3D-AJA			Kinect SDK			p-value**		
	Shoulder Flexion	Shoulder Abduction	Elbow Flexion	Shoulder Flexion	Shoulder Abduction	Elbow Flexion	Shoulder Flexion	Shoulder Abduction	Elbow Flexion
Sitting Self-selected	5.7 ± 5.0	5.7 ± 4.7	7.5 ± 7.8	9.2 ± 8.9	7.4 ± 7.4	14.6 ± 10.9	0.047*	0.249	0.002*
Sitting Ideal	6.1 ± 5.7	5.4 ± 4.4	6.0 ± 5.1	7.3 ± 7.3	7.4 ± 8.7	11.5 ± 12.3	0.287	0.070	< 0.001*
Sitting Poor	6.6 ± 5.6	5.6 ± 3.9	10.0 ± 6.7	7.1 ± 5.8	6.1 ± 4.5	27.3 ± 19.5	0.585	0.441	< 0.001*
Overall Sitting	6.2 ± 5.5	5.5 ± 4.3	7.8 ± 6.6	7.6 ± 7.2	6.9 ± 7.1	18.2 ± 16.8	0.041*	0.023*	< 0.001*
Standing Self-selected	6.5 ± 4.4	4.6 ± 3.7	6.1 ± 5.4	8.5 ± 6.5	4.3 ± 3.4	14.2 ± 10.8	0.126	0.698	< 0.001*
Standing Ideal	7.0 ± 5.4	5.1 ± 4.7	8.1 ± 7.9	8.6 ± 6.5	4.2 ± 3.1	17.7 ± 13.9	0.099	0.170	< 0.001*
Standing Poor	6.2 ± 6.3	4.6 ± 3.6	11.3 ± 11.7	8.5 ± 6.8	4.8 ± 4.0	28.5 ± 17.3	0.031*	0.669	< 0.001*
Overall Standing	6.6 ± 5.6	4.8 ± 4.1	9.0 ± 9.4	8.6 ± 6.6	4.5 ± 3.5	21.2 ± 15.9	0.002*	0.407	< 0.001*
Overall First Hour	6.4 ± 5.5	5.1 ± 4.2	8.4 ± 8.2	8.1 ± 6.9	5.7 ± 5.7	19.7 ± 16.4	< 0.001*	0.149	< 0.001*
Overall Second Hour	6.0 ± 5.9	6.8 ± 6.7	8.5 ± 7.9	8.8 ± 7.9	7.4 ± 7.7	14.4 ± 14.2	< 0.001*	0.440	< 0.001*
Overall	6.3 ± 5.7	5.6 ± 5.1	8.5 ± 8.1	8.3 ± 7.2	6.2 ± 6.4	18.2 ± 16.0	< 0.001*	0.113	< 0.001*

*denotes significance at $p < 0.05$.
**Independent sample *t*-test was used to compare the MAEs between the two methods.

Table 5
Pearson correlation (r) between calculated body joint angles and goniometry measurements.

	3D-AJA			Kinect SDK		
	Shoulder Flexion	Shoulder Abduction	Elbow Flexion	Shoulder Flexion	Shoulder Abduction	Elbow Flexion
Sitting Self-selected	0.86*	0.85*	0.79*	0.46*	0.82*	0.22
Sitting Ideal	0.78*	0.72*	0.90*	0.65*	0.06	0.42*
Sitting Poor	0.81*	0.66*	0.94*	0.76*	0.67*	0.34*
Overall Sitting	0.83*	0.77*	0.92*	0.68*	0.43*	0.36*
Standing Self-selected	0.76*	0.74*	0.82*	0.51*	0.56*	0.03
Standing Ideal	0.70*	0.52*	0.83*	0.53*	0.63*	0.24*
Standing Poor	0.64*	0.52*	0.67*	0.33*	0.37*	−0.11
Overall Standing	0.69*	0.53*	0.88*	0.45*	0.51*	0.18*
Overall First Hour	0.79*	0.77*	0.90*	0.61*	0.61*	0.30*
Overall Second Hour	0.84*	0.72*	0.84*	0.65*	0.64*	0.27*
Overall	0.81*	0.76*	0.89*	0.63*	0.63*	0.30*

*denotes significance at $p < 0.05$.

Table 6
Confusion matrices for the Random Forest models for the 3D-AJA and the Kinect SDK.

3D-AJA		Predicted Class					
		"1"	"2"	"3"	"4"	"5"	"7"
Actual Class	"1"	7	4	0	0	0	0
	"2"	2	201	27	0	0	0
	"3"	0	55	127	5	0	0
	"4"	0	5	16	56	9	1
	"5"	0	0	4	1	20	0
	"7"	0	0	0	0	0	2
Kinect SDK		Predicted Class					
		"1"	"2"	"3"	"4"	"5"	"7"
Actual Class	"1"	5	3	0	0	0	0
	"2"	1	166	33	0	0	0
	"3"	0	58	114	4	1	0
	"4"	0	15	12	45	11	0
	"5"	0	0	4	4	17	0
	"7"	0	0	0	0	0	2

Table 7
Performance metrics for the Random Forest models.

Class	**3D-AJA, Accuracy = 76.20%**				
	FP Rate	**TP Rate (Recall)**	**Precision**	**F1-score**	**G-mean**
"1"	0.004	0.636	0.778	0.700	0.796
"2"	0.205	0.874	0.758	0.812	0.834
"3"	0.132	0.679	0.730	0.704	0.768
"4"	0.013	0.644	0.903	0.752	0.797
"5"	0.017	0.800	0.690	0.741	0.887
"7"	0.002	1.000	0.667	0.800	0.999
Average	**0.062**	**0.772**	**0.754**	**0.752**	**0.847**
Weighted Avg.	**0.136**	**0.762**	**0.769**	**0.759**	**0.811**

Class	**Kinect SDK, Accuracy = 70.51%**				
	FP Rate	**TP Rate (Recall)**	**Precision**	**F1-score**	**G-mean**
"1"	0.002	0.625	0.833	0.714	0.790
"2"	0.258	0.830	0.686	0.751	0.785
"3"	0.154	0.644	0.699	0.671	0.738
"4"	0.019	0.542	0.849	0.662	0.729
"5"	0.026	0.680	0.586	0.630	0.814
"7"	0.000	1.000	1.000	1.000	1.000
Average	**0.077**	**0.720**	**0.776**	**0.738**	**0.809**
Weighted Avg.	**0.164**	**0.705**	**0.717**	**0.702**	**0.768**

minority classes, e.g., classes 4 and 5, and even the majority class 3. While precision and specificity are appropriate performance measures for problems that aim at minimizing false positives, and recall (sensitivity) for problems that aim at minimizing false negatives, using any of these metrics alone may not tell the whole story since a model may have high precision but low recall (and vice-versa), and low sensitivity and high specificity (and vice-versa). F1-scores and G-means combine the results of precision and recall, and sensitivity and specificity, respectively, by means of harmonic (for F1-score) and geometric (for G-mean) means in a way that balances out the concerns of minimizing all types of classification errors. In both cases (F1-score and G-means), the possible performance values range between 0 and 1, with higher values being an indication of better performance, i.e., fewer misclassifications.

5. Discussion

5.1. MAEs and correlation analysis

As Tables 4 and 5 show, overall, the 3D-AJA reduced measurement error and resulted in higher correlation to standard goniometry measurements as compared to the Kinect SDK. Consequently, the estimation of joint angles from the 3D-AJA were closer to the actual values provided by standard goniometry, which resulted in better performance during the determination of the RULA scores A (section 5.2) as it was observed for the Kinect SDK method. The results show that the estimation of body joint angles by the 3D-AJA has overall MAEs of $6.3^\circ \pm 5.7^\circ$ for shoulder flexion, $5.6^\circ \pm 5.1^\circ$ for shoulder abduction, and $8.5^\circ \pm 8.1^\circ$ for elbow flexion. Comparatively, the Kinect SDK performed worse, with MAEs of $8.3^\circ \pm 7.2^\circ$, $6.2^\circ \pm 6.4^\circ$, and $18.2^\circ \pm 16.0^\circ$ for shoulder flexion, shoulder abduction, and elbow flexion, respectively. These MAEs for the Kinect SDK are similar to errors previously reported for estimating shoulder flexion ($8.7^\circ \pm 5.9^\circ$ right/$9.1^\circ \pm 6.4^\circ$ left) and shoulder abduction ($14.8^\circ \pm 5.9^\circ$ right/$9.9^\circ \pm 4.6^\circ$ left) in individuals who were sitting [44]. A possible explanation for this verified worse performance compared to our algorithm might be due to the occlusions on the trunk caused by the adjustable desk in sitting and standing postures. As it is presented in Kar [65], Diego-Mas, and Alcaide-Marzal [35], the Kinect SDK has low accuracy when part of the body is not visible to the camera. No significant differences in terms of the MAEs were found for any of the assessed angles between sitting and standing positions for the 3D-AJA while for the Kinect SDK a significant difference was found between the sitting and standing positions for shoulder abduction. This difference in shoulder abduction might be due to the variances in the sitting and standing height of the participants. When sitting, the locations of the upper arms were lower in height relative to the Kinect camera resulting in fewer points captured by the depth channel of the Kinect camera for the upper arm, thereby influencing the assessment of shoulder abduction angles.

In addition to reducing measurement error as compared to the Kinect SDK, the 3D-AJA improved consistency in measurement estimation, demonstrating strong correlation to goniometric measures overall (i.e., 0.81, 0.76, 0.89 for shoulder flexion, shoulder abduction, and elbow flexion, respectively) across the three joints as compared to the weak to moderate correlations achieved by the Kinect SDK (i.e., 0.63, 0.63, 0.30 for shoulder flexion, shoulder abduction, and elbow flexion, respectively). The results for the second hour also support this finding and show that, for the condition in which the participants were completely free to select and adjust their working positions over time, the 3D-AJA correlated more strongly to the goniometer angles than the angles from the Kinect SDK method, which gives an indication of the ecological validity of the proposed method.

5.2. RULA upper limb risk classification

For the analysis of the ability of the three angles and the sitting/standing condition of the participants to determine the RULA score A (i.e., upper limb subscore), the most critical factor was related to the imbalanced distribution of the instances in the datasets among the possible classes of RULA score A (scores 1 through 9). The use of the SMOTE algorithm, however, proved effective as both F1-scores and G-means were above 0.700 for all classes in the 3D-AJA and 0.630 for all classes in the Kinect SDK. Additionally, as the confusion matrices in Table 6 show, most of the misclassifications happened between adjacent classes, e.g., classes 2 and 3. The reason behind this observation is twofold. First, individual RULA scores associated with each joint during RULA assessments are based on a continuum of possible angles relative to angle thresholds, which makes it possible for slight differences in angle estimates (i.e., 1-degree of error) from the automated methods (3D-AJA and Kinect SDK) to incorrectly place the score in the wrong RULA class. Second, in this study, only three angles from the automated algorithm were used to determine the RULA score A, whereas angles in the wrist and adjustments for other upper limb factors were included in the expert RULA observations, which can incorrectly place the score in the wrong RULA class as well.

Despite some limitations in data heterogeneity and using only three angles to train the classification models, the 3D-AJA data resulted in generally good risk assessment models relative to expert observations. Taking the Random Forest models depicted in Tables 6 and 7, it is possible to observe that, even in face of the imbalanced datasets used to build these models, the lowest F1-score for a single class in the model resulting from the data from the 3D-AJA is 0.700, with a micro average F1-score for all six classes of 0.759. Although the accuracy metric was not selected as an indicator of the quality of the models, Table 7 shows that the Random Forest model for the 3D-AJA dataset reached 76.20% accuracy in classification, which is a relatively good result if one considers that only a limited number of features were used to predict the RULA score A. It is likely possible to increase the performance of the classification models by adding other features involved in the determination of the RULA score A, especially with regards to wrist position. However, given the current performance, an automated framework that relies on data solely from the shoulder and elbow may adequately delineate risk, particularly because positioning of the wrist is likely to be highly dependent upon positioning of the proximal joints already being assessed.

5.3. Comparison of 3D-AJA with existing automated assessment methods

Although no comparisons were directly made between the 3D-AJA and other existing automated postural assessments in the literature due to the varied requirements, assumptions, and boundary conditions made during the development of each proposed method, some comparisons between the 3D-AJA and other existing automated assessment methods are made based on the summaries presented in Table 1 and the results presented in Tables 4 to 7. Although the 3D-AJA performed relatively worse than some of the listed automated assessment methods, the boundary conditions differed among the studies. In most cases, the proposed algorithms were based on ideal conditions in which no occlusion existed or, when occlusion occurred, it occurred in a restricted area of the subject's body. In the case of the 3D-AJA method described in this paper, the effects of occlusion were more significant since for most images part of the trunk and both legs were hidden from the Kinect camera. Additionally, some studies achieved high levels of accuracy but were based on a restricted number of postures on which the algorithms were trained and/or on lighting, clothing, and hair style requirements. In the 3D-AJA, the subjects were relatively free to select their working postures (except for the intervals when they were asked to sit in a bad or good posture during part of the first hour of data collection), wear their usual clothes, and keep their hair as they wish.

5.4. Practical implications of the results

A few considerations need to be made relative to the MAE results for the 3D-AJA in terms of its accuracy and practical implications. In clinical practice, it is common to limit the clinically significant error in angle measurement to $\pm 5.0^{\circ}$ [36,92], a threshold that was not met for most workstation conditions in the experiment. As Table 4 shows, the overall MAEs for all three angles of interest, shoulder flexion, shoulder abduction, and elbow flexion, were in the range $5.6^{\circ} \pm 5.1^{\circ}$ to $8.5^{\circ} \pm 8.1^{\circ}$ for the 3D-AJA. Added to that, the standard deviation values for all MAEs values listed in Table 4 were in the same order of magnitude of the MAE value and, on a few occasions, the standard deviation was bigger than the mean value. This means that the values of the errors of the angles from the 3D-AJA relative to the goniometer angles were spread around the mean and a relatively high variability can be expected in terms of the predicted angles by the model. In terms of the practical implications of these results on automated RULA assessments, when angle measurement error is high, there is a higher chance that individual RULA scores for different body joints would be underestimated/overestimated, thus resulting in incorrect individual RULA scores and, in the long term, increased risk of MSDs due to an inaccurate assessment of joint angles. Alternatively, when accurate measurements are made, and correct RULA scores are calculated, there is an increased chance of providing useful feedback to workers and implementing effective changes to the workplace, which can ultimately promote behavioral adaptations among office workers. In this sense, reducing the overall measurement errors of any proposed automated ergonomic assessment method is key for its usefulness in clinical practice. For RULA applications, specifically, because the method is based on angular thresholds, it tends to minimize the effects of noise, especially when the angles are not close to the class thresholds, thus leading to lower error rates as compared to methods that are based on the values of the joint angles alone [64].

Additionally, by allowing participants to adjust the workstation based on their preferences during the second hour of the data collection, this study provided preliminary ecological validity testing of the algorithm, something not done in any of the previous studies in automated ergonomic assessment in office environments. Although shoulder abduction error was slightly increased during this second hour, the average error remained lower than the Kinect SDK. These results provide strong impetus for further real-time, direct testing of the algorithm with workers in their office workspaces to identify additional improvements needed to confirm the utility for automation. Furthermore, in terms of its applicability to reduce the injury risk of workers, once developed, the application can be used as a personalized behavior change tool that can inform workers of potential ergonomic risks throughout their daily work, which can help workers to adjust their postures and, thus, reduce ergonomic risks. If used along with more traditional ergonomic assessments, in which an ergonomist assesses the workplace and suggests changes, this tool can support the promotion of the suggested changes by providing timely and continuous feedback to the workers. Finally, in addition to monitoring office workers' postures and minimizing the

impact of musculoskeletal disorders caused by inappropriate work postures, the 3D-AJA can benefit other fields as well. Potential applications include the use of automated assessments in telemedicine applications that involve elderly people, post-surgical patients, and physical therapy patients, for example.

5.5. Limitations of the study and future work

Some limitations were inherent to the design of this office-based validation study. First, although the Kinect camera was placed in front of the participants during the experiment, there were times when upper body segments became self-occluded, thus reducing the performance of the algorithm. Future studies could focus on varying the number of cameras used or the camera positioning relative to the worker to minimize occlusions. Second, while the algorithm was tested using data from 20 different participants who had a variety of body habitus, clothing, hair, and other behavioral tendencies, observations were only made during a selected number of times across 2 h. Considering the average 8-hour daily work time, longer hours of posture monitoring and assessment are necessary to fully examine the accuracy of the algorithm. Although participants of the study included males and females, with ages ranging from 20 to 50 years old, and from various ethnicities, the sample size of the study was not sufficiently large to evaluate potential differences in the performance of the 3D-AJA based on differences in terms of gender, age, or ethnicity. Next, this study only investigated positioning of the shoulders and arms, and further development and testing are needed to develop a robust, full-body ergonomic assessment of office workers that includes other key postures and positions, particularly in the neck, trunk, and legs (RULA score B) to allow for a complete RULA assessment of postural risks. Also, privacy issues related to using cameras in the workplace might be a concern for office workers. Although the Kinect camera is non-intrusive compared to wearable sensors, people might not feel comfortable being monitored at work. Processing the data without saving collected images might be helpful to alleviate this problem. Finally, installing a Kinect to each workstation may not be feasible. There are, however, cheaper RGB-D camera alternatives, which can bring down the costs in cases when the presented methodology is to be employed in a real office space with many workstations. In terms of computational performance, as the 3D-AJA relies on complex computer vision algorithms, the computation times may increase in case a less powerful computer is used. As a potential solution, developing a cloud version of the application can reduce the need for more powerful computers in each workstation. Another important consideration is that, in this study, the feedback requirements of the application, in terms of frequency and type, were not evaluated and were left as suggestions for future research. Also, a potential improvement in terms of storage requirements and computational performance can be achieved by downsampling the resulting point cloud for each frame before computing the joint angles of interest. During the testing and validation of the 3D-AJA, however, the impacts of using a downsampled point cloud relative to the accuracy of the predicted joint angles and posterior RULA scoring were not investigated and are left as suggestions for future work.

6. Conclusion

The objective of this study was to develop and test an automated ergonomic assessment algorithm, the 3D-AJA, for office workers in office environments. Results showed that compared to goniometry measurements, the joint angles calculated by our algorithm has MAEs of $6.3^\circ \pm 5.7^\circ$ for shoulder flexion, $5.6^\circ \pm 5.1^\circ$ for shoulder abduction, and $8.5^\circ \pm 8.1^\circ$ for elbow flexion. The 3D-AJA outperformed Kinect SDK body joint capture method for estimating all three selected angles with significant differences in terms of shoulder flexion and elbow flexion angles. In terms of the resulting classification models for the determination of the RULA score A, the dataset from the 3D-AJA resulted in better classification models for all RULA score A classes included in the datasets. Despite these datasets being composed of highly imbalanced classes, the performance of the resulting classification models achieved relatively high results, with F1-scores reaching 0.759 and G-means reaching 0.814. Relatively good results were also achieved for individual classes and, for the Random Forest models, F1-score of at least 0.700 and G-mean of at least 0.768, even in face of high-class imbalances, the limited number of features in the dataset, i.e., only three angles and sitting/standing condition, and occlusion effects from the desk. This study provides a solid foundation for future work to provide a full-body ergonomic assessment for office workers. To perform longitudinal studies on office worker postures, this algorithm could be a cost-effective and efficient tool for future research to gather continuous postural data for an extended duration of posture monitoring and the effect of work postures on office worker health.

Declaration of Competing Interest

The authors declare that they have no known competing financial interests or personal relationships that could have appeared to influence the work reported in this paper.

Acknowledgments

The authors would like to thank Vivek Rajaram Mishra who assisted in data collection and the initial development of computer vision algorithms, and Jody Liu who dedicated extensive hours to the observational analyses in this work.

Funding

This research was supported by National Science Foundation [grant #1763134] and the U.S. Army Research Office [grant #W911NF2020053]. Any opinions, findings, and conclusions, or recommendations expressed in this material are those of the authors and do not necessarily reflect the views of the National Science Foundation or U.S. Army.

References

[1] C. Tudor-Locke, C. Leonardi, W.D. Johnson, P.T. Katzmarzyk, Time spent in physical activity and sedentary behaviors on the working day: The American Time Use Survey, J. Occup. Environ. Med. 53 (12) (2011) 1382–1387, https://doi.org/10.1097/JOM.0b013e31823c1402.

[2] A.H.Y. Chu, S.H.X. Ng, C.S. Tan, A.M. Win, D. Koh, F. Müller-Riemenschneider, A systematic review and meta-analysis of workplace intervention strategies to reduce sedentary time in white-collar workers, Obes. Rev. 17 (5) (2016) 467–481, https://doi.org/10.1111/obr.12388.

[3] S. Parry, L. Straker, The contribution of office work to sedentary behaviour associated risk, BMC Public Health 13 (2013) 1–10, https://doi.org/10.1186/1471-2458-13-296. Article number: 296.

[4] C.G. Ryan, P.M. Grant, P.M. Dall, M.H. Granat, Sitting patterns at work: Objective measurement of adherence to current recommendations, Ergonomics 54 (6) (2011) 531–538, https://doi.org/10.1080/00140139.2011.570458.

[5] J.A. Cole, M.A. Tully, M.E. Cupples, "They should stay at their desk until the work's done": a qualitative study examining perceptions of sedentary behaviour in a desk-based occupational setting Public Health, BMC Res. Notes. 8 (2015) 1–9, https://doi.org/10.1186/s13104-015-1670-2. Article number: 683.

[6] F. Ricci, P. Izzicupo, F. Moscucci, S. Sciomer, S. Maffei, A. Di Baldassarre, A. V. Mattioli, S. Gallina, Recommendations for Physical Inactivity and Sedentary Behavior During the Coronavirus Disease (COVID-19) Pandemic, Front. Public Heal. 8 (2020) 8–11, https://doi.org/10.3389/fpubh.2020.00199. Article number: 199.

[7] Y. Xiao, B. Becerik-Gerber, G. Lucas, S.C. Roll, Impacts of Working From Home During COVID-19 Pandemic on Physical and Mental Well-Being of Office Workstation Users, J. Occup. Environ. Med. 63 (3) (2021) 181–190, https://doi.org/10.1097/JOM.0000000000002097.

[8] M. Awada, G. Lucas, B. Becerik-Gerber, S. Roll, Working from home during the COVID-19 pandemic: Impact on office worker productivity and work experience, Work 69 (4) (2021) 1171–1189, https://doi.org/10.3233/WOR-210301.

[9] J.Y. Chau, A.C. Grunseit, T. Chey, E. Stamatakis, W.J. Brown, C.E. Matthews, A. E. Bauman, H.P. van der Ploeg, O. Gorlova, Daily sitting time and all-cause mortality: a meta-analysis, PLoS ONE 8 (11) (2013), https://doi.org/10.1371/journal.pone.0080000.

[10] S. Eltayeb, J.B. Staal, A. Hassan, R.A. De Bie, Work related risk factors for neck, shoulder and arms complaints: A cohort study among Dutch computer office workers, J. Occup. Rehabil. 19 (2009) 315–322, https://doi.org/10.1007/s10926-009-9196-x.

[11] F. Gerr, M. Marcus, C. Ensor, D. Kleinbaum, S. Cohen, A. Edwards, E. Gentry, D. J. Ortiz, C. Monteilh, A prospective study of computer users: I. Study design and incidence of musculoskeletal symptoms and disorders, Am. J. Ind. Med. 41 (4) (2002) 221–235, https://doi.org/10.1002/ajim.10066.

[12] U.S. Bureau of Labor Statistics, Case and Demographic Characteristics for Work-related Injuries and Illnesses Involving Days Away From Work, (2021). https://www.bls.gov/iif/oshwc/osh/case/cd_r66_2020.htm (accessed December 17, 2021).

[13] F. Lötters, A. Burdorf, Prognostic factors for duration of sickness absence due to musculoskeletal disorders, Clin. J. Pain. 22 (2) (2006) 212–221, https://doi.org/10.1097/01.ajp.0000154047.30155.72.

[14] B.B. Arnetz, B. Sjögren, B. Rydéhn, R. Meisel, Early workplace intervention for employees with musculoskeletal-related absenteeism: A prospective controlled intervention study, J. Occup. Environ. Med. 45 (5) (2003) 499–506, https://doi.org/10.1097/01.jom.0000063628.37065.45.

[15] R. Pohling, G. Buruck, K.L. Jungbauer, M.P. Leiter, Work-related factors of presenteeism: The mediating role of mental and physical health, J. Occup. Health Psychol. 21 (2) (2016) 220–234, https://doi.org/10.1037/a0039670.

[16] M. Ardahan, H. Simsek, Analyzing musculoskeletal system discomforts and risk factors in computer-using office workers, Pakistan, J Med. Sci. 32 (6) (2016) 1425–1429. https://doi.org/10.12669/pjms.326.11436.

[17] L.K. Karlqvist, E. Bernmark, L. Ekenvall, M. Hagberg, A. Isaksson, T. Rostö, Computer mouse position as a determinant of posture, muscular load and perceived exertion, Scand. J. Work. Environ. Heal. 24 (1) (1998) 62–73, https://doi.org/10.5271/sjweh.279.

[18] G.C. David, Ergonomic methods for assessing exposure to risk factors for work-related musculoskeletal disorders, Occup. Med. (Chic. Ill) 55 (3) (2005) 190–199, https://doi.org/10.1093/occmed/kqi082.

[19] P. Spielholz, B. Silverstein, M. Morgan, H. Checkoway, J. Kaufman, Comparison of self-report, video observation and direct measurement methods for upper extremity musculoskeletal disorder physical risk factors, Ergonomics 44 (6) (2001) 588–613, https://doi.org/10.1080/00140130118050.

[20] L. McAtamney, E. Nigel Corlett, RULA: a survey method for the investigation of work-related upper limb disorders, Appl. Ergon. 24 (2) (1993) 91–99, https://doi.org/10.1016/0003-6870(93)90080-S.

[21] N.D. Gilson, N. Ng, T.G. Pavey, G.C. Ryde, L. Straker, W.J. Brown, Project Energise: Using participatory approaches and real time computer prompts to reduce occupational sitting and increase work time physical activity in office workers, J. Sci. Med. Sport. 19 (11) (2016) 926–930, https://doi.org/10.1016/j.jsams.2016.01.009.

[22] N. Shrestha, K.T. Kukkonen-Harjula, J.H. Verbeek, S. Ijaz, V. Hermans, Z. Pedisic, Workplace interventions for reducing sitting at work, Cochrane Database Syst. Rev. (6) (2018) CD010912, https://doi.org/10.1002/14651858.CD010912.pub4.

[23] R. Leyshon, K. Chalova, L. Gerson, A. Savtchenko, R. Zakrzewski, A. Howie, L. Shaw, Ergonomic interventions for office workers with musculoskeletal disorders: a systematic review, Work 35 (3) (2010) 335–348, https://doi.org/10.3233/WOR-2010-0994.

[24] E. Barkallah, J. Freulard, M.J.D. Otis, S. Ngomo, J.C. Ayena, C. Desrosiers, Wearable devices for classification of inadequate posture at work using neural networks, Sensors (Switzerland) 17 (9) (2017) 1–24, https://doi.org/10.3390/s17092003.

[25] L. Peppoloni, A. Filippeschi, E. Ruffaldi, Assessment of task ergonomics with an upper limb wearable device, in: 22nd Mediterranean Conference on Control and Automation, 2014, pp. 340–345, https://doi.org/10.1109/MED.2014.6961394.

[26] S.L. Delp, F.C. Anderson, A.S. Arnold, P. Loan, A. Habib, C.T. John, E. Guendelman, D.G. Thelen, OpenSim: open-source software to create and analyze dynamic simulations of movement, IEEE Trans. Biomed. Eng. 54 (11) (2007) 1940–1950, https://doi.org/10.1109/TBME.2007.901024.

[27] P. Plantard, H.P.H. Shum, A.S. Le Pierres, F. Multon, Validation of an ergonomic assessment method using Kinect data in real workplace conditions, Appl. Ergon. 65 (2017) 562–569, https://doi.org/10.1016/j.apergo.2016.10.015.

[28] A. Altieri, S. Ceccacci, A. Talipu, M. Mengoni, A Low Cost Motion Analysis System Based on RGB Cameras to Support Ergonomic Risk Assessment in Real Workplaces, in: Proceedings of the ASME 2020 International Design Engineering Technical Conferences and Computers and Information in Engineering Conference. Volume 9: 40th Computers and Information in Engineering Conference (CIE), 2020, https://doi.org/10.1115/DETC2020-22308. Article number: V009T09A067.

[29] A. Abobakr, D. Nahavandi, J. Iskander, M. Hossny, S. Nahavandi, M. Smets, RGB-D human posture analysis for ergonomic studies using deep convolutional neural network, IEEE Int. Conf. Syst. Man, Cybern. (2017) 2885–2890, https://doi.org/10.1109/SMC.2017.8123065.

[30] J. Krüger, T.D. Nguyen, Automated vision-based live ergonomics analysis in assembly operations, CIRP Ann. - Manuf. Technol. 64 (1) (2015) 9–12, https://doi.org/10.1016/j.cirp.2015.04.046.

[31] J. Seo, S. Lee, Automated postural ergonomic risk assessment using vision-based posture classification, Autom. Constr. 128 (2021) 1–12, https://doi.org/10.1016/j.autcon.2021.103725. Article number: 103725.

[32] R.-J. Dzeng, H.-H. Hsueh, C.W. Ho, Automated Posture Assessment for construction workers, in: 40th International Convention on Information and Communication Technology, Electronics and Microelectronics (MIPRO), IEEE, 2017, pp. 1027–1031, https://doi.org/10.23919/MIPRO.2017.7973575.

[33] L.C. Büker, F. Zuber, A. Hein, S. Fudickar, Hrdepthnet: Depth image-based marker-less tracking of body joints, Sensors (Basel) 21 (4) (2021) 1–17, https://doi.org/10.3390/s21041356. Aricle number: 1356.

[34] J. Shotton, A. Fitzgibbon, M. Cook, T. Sharp, M. Finocchio, R. Moore, A. Kipman, A. Blake, Real-time human pose recognition in parts from single depth images, in: IEEE Conference on Computer Vision and Pattern Recognition (CVPR), 2011, pp. 1297–1304, https://doi.org/10.1109/CVPR.2011.5995316.

[35] J.A. Diego-Mas, J. Alcaide-Marzal, Using Kinect™ sensor in observational methods for assessing postures at work, Appl. Ergon. 45 (4) (2014) 976–985, https://doi.org/10.1016/j.apergo.2013.12.001.

[36] M.E. Huber, A.L. Seitz, M. Leeser, D. Sternad, Validity and reliability of Kinect skeleton for measuring shoulder joint angles: a feasibility study, Physiother. (United Kingdom) 101 (4) (2015) 389–393, https://doi.org/10.1016/j.physio.2015.02.002.

[37] L. Cai, Y.e. Ma, S. Xiong, Y. Zhang, Validity and Reliability of Upper Limb Functional Assessment Using the Microsoft Kinect V2 Sensor, Appl. Bionics Biomech. (2019) 1–14, https://doi.org/10.1155/2019/7175240. Aricle number: 7175240.

[38] R.P. Kuster, B. Heinlein, C.M. Bauer, E.S. Graf, Accuracy of KinectOne to quantify kinematics of the upper body, Gait Posture 47 (2016) 80–85, https://doi.org/10.1016/j.gaitpost.2016.04.004.

[39] S.H. Lee, C. Yoon, S.G. Chung, H.C. Kim, Y. Kwak, H.-W. Park, K. Kim, A. Nógrádi, Measurement of shoulder range of motion in patients with adhesive capsulitis using a Kinect, PLoS ONE 10 (6) (2015), https://doi.org/10.1371/journal.pone.0129398. Aricle number: e0129398.

[40] V. Bhatia, P. Kalra, J.S. Randhawa, Upper body postural analysis in sitting workplace environment using microsoft kinect v2 sensor, Smart Innov. Syst. Technol. 135 (2019) 575–586, https://doi.org/10.1007/978-981-13-5977-4_49.

[41] B. Liu, Y. Li, S. Zhang, X. Ye, Healthy human sitting posture estimation in RGB-D scenes using object context, Multimed. Tools Appl. 76 (2017) 10721–10739, https://doi.org/10.1007/s11042-015-3189-x.

[42] D.J. Shin, M.S. Kim, W. Song, S.D. Min, M. Hong, Implementation of sitting posture monitoring system with kinect, in: Advanced Multimedia and Ubiquitous Engineering. FutureTech MUE 2017. Lecture Notes in Electrical Engineering, vol. 448, 2017, https://doi.org/10.1007/978-981-10-5041-1_26.

[43] S. Teeravarunyou, Development of Computer Aided Posture Analysis for Rapid Upper Limb Assessment with Ranged Camera, in: 3rd South East Asian Network of Ergonomics Societies International Conference, 2014, pp. 1–6.

[44] X. Xu, M. Robertson, K.B. Chen, J. hua Lin, R.W. McGorry, Using the Microsoft Kinect™ to assess 3-D shoulder kinematics during computer use, Appl. Ergon. 65 (2017) 418–423, https://doi.org/10.1016/j.apergo.2017.04.004.

[45] S. Maheronnaghsh, J. Santos, M. Vaz, Methods of posture analysis for computer workers, Int. J. Occup. Environ. Saf. 2 (2) (2018) 41–49, https://doi.org/10.24840/2184-0954_002.002_0005.

[46] N.P. Pronk, A.S. Katz, M. Lowry, J.R. Payfer, Reducing occupational sitting time and improving worker health: the Take-a-Stand Project, 2011, Prev. Chronic Dis. 9 (2012) 1–9, https://doi.org/10.5888/pcd9.110323.

[47] J.L. Bruno, Z. Li, M. Trudeau, S.M. Raina, J.T. Dennerlein, A single video camera postural assessment system to measure rotation of the shoulder during computer use, J. Appl. Biomech. 28 (3) (2012) 343–348, https://doi.org/10.1123/jab.28.3.343.

[48] Z. Ding, W. Li, P. Ogunbona, L. Qin, A real-time webcam-based method for assessing upper-body postures, Mach. Vis. Appl. 30 (5) (2019) 833–850, https://doi.org/10.1007/s00138-019-01033-9.

[49] G. Marfia, M. Roccetti, A practical computer based vision system for posture and movement sensing in occupational medicine, Multimed. Tools Appl. 76 (2017) 8109–8129, https://doi.org/10.1007/s11042-016-3469-0.

[50] P. Westfeld, H.G. Maas, O. Bringmann, D. Gröllich, M. Schmauder, Automatic techniques for 3D reconstruction of critical workplace body postures from range imaging data, ISPRS J. Photogramm. Remote Sens. 85 (2013) 56–65, https://doi.org/10.1016/j.isprsjprs.2013.08.004.

[51] A. Abobakr, D. Nahavandi, M. Hossny, J. Iskander, M. Attia, S. Nahavandi, M. Smets, RGB-D ergonomic assessment system of adopted working postures, Appl. Ergon. 80 (2019) 75–88, https://doi.org/10.1016/j.apergo.2019.05.004.

[52] I. Halim, R.Z. Radin Umar, N. Ahmad, M.R. Jamli, M.S. Syed Mohamed, T.M. M. Albawab, M.H. Lim Abdullah, V. Padmanathan, Usability Study of Integrated RULA-KinectTM System for Work Posture Assessment, Int. J. Integr. Eng. 10 (8) (2018), https://doi.org/10.30880/ijie.2018.10.08.027.

[53] P. Plantard, H.P. Hubert, F. Multon, Filtered pose graph for efficient kinect pose reconstruction, Multimed. Tools Appl. 76 (2017) 4291–4312, https://doi.org/10.1007/s11042-016-3546-4.

[54] M. Tarabini, M. Marinoni, M. Mascetti, P. Marzaroli, F. Corti, H. Giberti, P. Mascagni, A. Villa, T. Eger, Real-time monitoring of the posture at the workplace using low cost sensors, in: Proceedings of the 20th Congress of the International Ergonomics Association (IEA 2018). Advances in Intelligent Systems and Computing, vol. 820, 2019, pp. 678–688, https://doi.org/10.1007/978-3-319-96083-8_85.

[55] M. Bortolini, M. Faccio, M. Gamberi, F. Pilati, Motion Analysis System (MAS) for production and ergonomics assessment in the manufacturing processes, Comput. Ind. Eng. 139 (2020) 105485, https://doi.org/10.1016/j.cie.2018.10.046.

[56] A. Abobakr, M. Hossny, S. Nahavandi, Body joints regression using deep convolutional neural networks, 2016 IEEE Int. Conf. Syst. Man, Cybern. SMC 2016 - Conf. Proc. (2017) 3281–3287. https://doi.org/10.1109/SMC.2016.7844740.

[57] H. Haggag, M. Hossny, S. Nahavandi, D. Creighton, Real time ergonomic assessment for assembly operations using kinect, in: 2013 UKSim 15th

International Conference on Computer Modelling and Simulation, 2013, pp. 495–500, https://doi.org/10.1109/UKSim.2013.105.
[58] S.J. Ray, J. Teizer, Real-time construction worker posture analysis for ergonomics training, Adv. Eng. Informatics. 26 (2) (2012) 439–455, https://doi.org/10.1016/j.aei.2012.02.011.
[59] R.J. Dzeng, Y.-P. Chiang, K. Watanabe, H.H. Hsueh, Marker-Less Based Detection of Repetitive Awkward Postures for Construction Workers, 2018 Int. Acad. Res. Conf. Vienna. (2018) 75–83.
[60] W. Cao, J. Zhong, G. Cao, Z. He, Physiological Function Assessment Based on Kinect V2, IEEE Access 7 (2019) 105638–105651, https://doi.org/10.1109/ACCESS.2019.2932101.
[61] V.M. Manghisi, A.E. Uva, M. Fiorentino, V. Bevilacqua, G.F. Trotta, G. Monno, Real time RULA assessment using Kinect v2 sensor, Appl. Ergon. 65 (2017) 481–491, https://doi.org/10.1016/j.apergo.2017.02.015.
[62] P. Plantard, E. Auvinet, A.S. Le Pierres, F. Multon, Pose estimation with a kinect for ergonomic studies: Evaluation of the accuracy using a virtual mannequin, Sensors (Switzerland). 15 (1) (2015) 1785–1803, https://doi.org/10.3390/s150101785.
[63] F. Mohammadipour, M. Pourranjbar, S. Naderi, F. Rafie, Work-related Musculoskeletal Disorders in Iranian Office Workers: Prevalence and Risk Factors, J. Med. Life. 11 (4) (2018) 328–333, https://doi.org/10.25122/jml-2018-0054.
[64] P. Plantard, H.P.H. Shum, F. Multon, Usability of Corrected Kinect Measurement for Ergonomic Evaluation in Constrained Environment, Int. J. Hum. Factors Model. Simul. 5 (4) (2017) 338–353, https://doi.org/10.1504/IJHFMS.2017.087018.
[65] A. Kar, Skeletal Tracking using Microsoft Kinect The Microsoft Kinect sensor, Methodology. 1–11 (2010).
[66] Y. Fujimoto, K. Fujita, Depth-Based Human Detection Considering Postural Diversity and Depth Missing in Office Environment, IEEE Access 7 (2019) 12206–12219, https://doi.org/10.1109/ACCESS.2019.2892197.
[67] L.G. Wiedemann, R. Planinc, M. Kampel, Ergonomic-Monitoring of office workplaces using Kinect, in: Ambient Assisted Living and Daily Activities. IWAAL 2014. Lecture Notes in Computer Science, vol. 8868, 2014, pp. 27–278, https://doi.org/10.1007/978-3-319-13105-4_40.
[68] L. Yao, W. Min, H. Cui, A new kinect approach to judge unhealthy sitting posture based on neck angle and torso angle, in: International Conference on Image and Graphics, 2017, pp. 340–350, https://doi.org/10.1007/978-3-319-71607-7_30.
[69] S.K. McCrady, J. Levine, Sedentariness at work: how much do we really sit? Obesity 17 (11) (2009) 2103–2105, https://doi.org/10.1038/oby.2009.117.
[70] L. Li, T. Martin, X. Xu, A novel vision-based real-time method for evaluating postural risk factors associated with musculoskeletal disorders, Appl. Ergon. 87 (2020) 103138, https://doi.org/10.1016/j.apergo.2020.103138.
[71] L. Wang, D.Q. Huynh, P. Koniusz, A Comparative Review of Recent Kinect-Based Action Recognition Algorithms, IEEE Trans. Image Process. 29 (2020) 15–28, https://doi.org/10.1109/TIP.2019.2925285.
[72] V. Belagiannis, A. Zisserman, Recurrent Human Pose Estimation, in: 12th IEEE International Conference on Automatic Face & Gesture Recognition (FG 2017), 2017, pp. 468–475, https://doi.org/10.1109/FG.2017.64.
[73] S.E. Wei, V. Ramakrishna, T. Kanade, Y. Sheikh, Convolutional pose machines, in: 2016 IEEE Conference on Computer Vision and Pattern Recognition (CVPR), 2016, pp. 4724–4732, https://doi.org/10.1109/CVPR.2016.511.
[74] Z. Cao, T. Simon, S.E. Wei, Y. Sheikh, Realtime multi-person 2D pose estimation using part affinity fields, in: Proceedings of the IEEE Conference on Computer Vision and Pattern Recognition (CVPR), 2017, pp. 1302–1310, https://doi.org/10.48550/ARXIV.1611.08050.
[75] L.C. Chen, G. Papandreou, I. Kokkinos, K. Murphy, A.L. Yuille, DeepLab: Semantic Image Segmentation with Deep Convolutional Nets, Atrous Convolution, and Fully Connected CRFs, IEEE Trans. Pattern Anal. Mach. Intell. 40 (4) (2018) 834–848, https://doi.org/10.1109/TPAMI.2017.2699184.
[76] H.S. Fang, G. Lu, X. Fang, J. Xie, Y.W. Tai, C. Lu, Weakly and Semi Supervised Human Body Part Parsing via Pose-Guided Knowledge Transfer, in: 2018 IEEE/CVF Conference on Computer Vision and Pattern Recognition (CVPR), 2018, pp. 70–78, https://doi.org/10.1109/CVPR.2018.00015.
[77] P. Jafarzadeh, P. Virjonen, P. Nevalainen, F. Farahnakian, J. Heikkonen, Pose Estimation of Hurdles Athletes using OpenPose, in: 2021 International Conference on Electrical, Computer, Communications and Mechatronics Engineering (ICECCME), 2021, pp. 1–6, https://doi.org/10.1109/ICECCME52200.2021.9591066.
[78] O. Aanuoluwapo, P. Frederick, Construction Worker Posture Estimation Using OpenPose, in: Construction Research Congress, 2020, pp. 556–564, https://doi.org/10.1061/9780784482872.060.
[79] MathWorks, pcfromkinect: Point cloud from Kinect for Windows (2020). https://www.mathworks.com/help/vision/ref/pcfromkinect.html (Accessed 25 June 2020).
[80] M. Mary Synthuja Jain Preetha, L. Padma Suresh, M. John Bosco, Image segmentation using seeded region growing, in: 012 International Conference on Computing, Electronics and Electrical Technologies (ICCEET), 2012, pp. 576–583, https://doi.org/10.1109/ICCEET.2012.6203897.
[81] H.M. Pendleton, W. Schultz-Krohn, Pedretti's occupational therapy : practice skills for physical dysfunction, 8th ed., Elsevier, Missouri, 2018.
[82] G. Wu, F.C.T. Van Der Helm, H.E.J. Veeger, M. Makhsous, P. Van Roy, C. Anglin, J. Nagels, A.R. Karduna, K. McQuade, X. Wang, F.W. Werner, B. Buchholz, ISB recommendation on definitions of joint coordinate systems of various joints for the reporting of human joint motion - Part II: Shoulder, elbow, wrist and hand, J. Biomech. 38 (5) (2005) 981–992, https://doi.org/10.1016/j.jbiomech.2004.05.042.
[83] N.V. Chawla, K.W. Bowyer, L.O. Hall, W.P. Kegelmeyer, SMOTE: Synthetic Minority over-Sampling Technique, J. Artif. Int. Res. 16 (2002) 321–357, https://doi.org/10.1613/jair.953.
[84] B. Krawczyk, M. Woźniak, F. Herrera, Weighted one-class classification for different types of minority class examples in imbalanced data, in: 2014 IEEE Symposium on Computational Intelligence and Data Mining (CIDM), 2014, pp. 337–344, https://doi.org/10.1109/CIDM.2014.7008687.
[85] N.V. Chawla, in: Data Mining and Knowledge Discovery Handbook, Springer-Verlag, New York, 2005, pp. 853–867.
[86] H. He, E.A. Garcia, Learning from Imbalanced Data, IEEE Trans. Knowl. Data Eng. 21 (9) (2009) 1263–1284, https://doi.org/10.1109/TKDE.2008.239.
[87] A. Agrawal, H.L. Viktor, E. Paquet, SCUT: Multi-class imbalanced data classification using SMOTE and cluster-based undersampling, in: 7th International Joint Conference on Knowledge Discovery, Knowledge Engineering and Knowledge Management (IC3K), 2015, pp. 226–234.
[88] E. Frank, M.A. Hall, I.H. Witten. The WEKA Workbench. Online Appendix for "Data Mining: Practical Machine Learning Tools and Techniques, 4th ed., Morgan Kaufmann, 2016, pp. 1–128. https://www.cs.waikato.ac.nz/ml/weka/Witten_et_al_2016_appendix.pdf.
[89] X. Zhu, I. Davidson. Knowledge*Discovery and Data Mining: Challenges and Realities*, IGI Global Publisher, 2007, https://doi.org/10.4018/978-1-59904-252-7.
[90] L.A. Jeni, J.F. Cohn, F.D. La Torre, Facing Imbalanced Data–Recommendations for the Use of Performance Metrics, in: 2013 Humaine Association Conference on Affective Computing and Intelligent Interaction, 2013, pp. 245–251, https://doi.org/10.1109/ACII.2013.47.
[91] N. Japkowicz, Assessment Metrics for Imbalanced Learning, first ed., Wiley, Hoboken, NJ, USA, 2013, pp. 187–206.
[92] V. Macionis, Reliability of the standard goniometry and diagrammatic recording of finger joint angles: a comparative study with healthy subjects and non-professional raters, BMC Musculoskelet. Disord. 14 (2013) 17, https://doi.org/10.1186/1471-2474-14-17.